

Nanohertz Gravitational Waves from Axion Domain Walls Coupled to QCD

Naoya Kitajima^{1,2}, Junseok Lee², Kai Murai²,
Fuminobu Takahashi², Wen Yin²

¹*Frontier Research Institute for Interdisciplinary Sciences, Tohoku University, Sendai,
Miyagi 980-8578 Japan*

²*Department of Physics, Tohoku University, Sendai, Miyagi 980-8578, Japan*

Abstract

We show that the recently reported NANOGrav, EPTA, PPTA, and CPTA data suggesting the existence of stochastic gravitational waves in the nanohertz region can be explained by axion domain walls coupled to QCD. In this scenario, the non-perturbative effects of QCD generate a temperature-dependent bias for the domain wall around the QCD phase transition, leading to an immediate collapse of the domain walls. We perform dedicated lattice simulations of the axion domain walls, taking into account the temperature dependence of the bias, to estimate the gravitational waves emitted during the domain wall annihilation process. We also discuss the future prospects for accelerator-based searches for the axion and the potential for the formation and detection of primordial black holes.

1 Introduction

There are various symmetries in physics beyond the Standard Model, and their spontaneous breaking during the evolution of the universe generates various topological defects [1–3] (see Ref. [4] for reviews). Provided that these symmetries are exact or preserved with high accuracy, the topological defects are stable and, once formed, can persist in the universe for a long time, thereby influencing the subsequent evolution of the universe. Topological defects play an important role in extracting information about physics beyond the Standard Model from cosmological observations, as they carry information about UV theory at extremely high energies. In particular, gravitational waves (GWs) are known to be emitted by the evolution and collapse of topological defects whose energy is spatially localized.

In this paper, we study GWs generated by domain walls (DWs) - created by spontaneous breaking of discrete symmetries - in scenarios where they are destabilized and collapse by explicit breaking of discrete symmetries [3, 5–12]. The GWs resulting from DW annihilation are characterized by their peak frequency and peak height. The peak frequency is determined by the timing of the DW annihilation, which can be used to extract the information of the UV physics (see e.g., Refs. [13–18]). The peak height depends on the energy density of the DWs at the decay. In most of the previous literature on the GWs generated by DW annihilation, the tension and the potential bias are treated as independent parameters, and in particular, the bias is often assumed to be a constant parameter. In this case, the peak frequency is determined by the balance between the tension and the potential bias. Instead, we propose here a scenario in which the DWs annihilate at a more or less fixed time, thanks to the temperature-dependent potential bias, which gives a more definite prediction about the peak frequency of the produced GWs.

As a candidate for DWs, we consider axion DWs. Axions, whose existence is strongly suggested by string theory, have attracted much attention in recent years and have been actively studied both theoretically and experimentally in various contexts, including dark matter, dark energy, and inflation. One of the features of axions is the periodicity of the potential, which naturally includes DW configurations.

We focus on the evolution of axion DWs when the axion is coupled to Standard Model gauge bosons, in particular gluons. In this case, due to the non-perturbative effects of QCD, a temperature-dependent explicit symmetry breaking is expected to grow as the temperature of the universe approaches the QCD scale, $T_{\text{QCD}} \sim 100$ MeV, leading to the decay of DWs around that time. While the potential bias is usually assumed to be a constant, in our scenario the potential bias is negligibly small well above the QCD scale, but rapidly increases

as the temperature approaches T_{QCD} . Thus, for the DW tension in a certain range, the DWs necessarily collapse near the QCD scale temperature, T_{QCD} . Therefore, this scenario predicts a very specific frequency range of GWs associated with the DW annihilation, which falls in the range of about $\mathcal{O}(1 - 10)$ nHz [17, 18]. This is within the sensitivity range of the pulsar timing array.

Very recently, the NANOGrav, EPTA, PPTA, and CPTA groups published data showing the detection of stochastic GW background in the $\mathcal{O}(1 - 10)$ nHz frequency band [19–22]. Supermassive black holes are a strong candidate for the origin of the GWs in this frequency range, and other new physics explanations are also possible such as the first-order phase transition in a hidden sector [23, 24] (see Ref. [25] and references therein for other possibilities). Among various possibilities, the above scenario that the QCD phase transition triggered the collapse of axion DWs is very attractive because it naturally explains the detected frequency range [17, 18].

We note that numerical calculations of GWs resulting from DW collapse, and the fitting models developed for them, have not considered the potential bias in solving for DW evolution [8, 10]. Instead, the bias has only been used as a parameter to determine the timing of the collapse. This timing has been evaluated when the DW tension and the bias are equal. The fitting model based on these results has been used in much of the literature. In reality, however, the collapse of the DWs takes a finite amount of time. It is therefore necessary to evaluate the GWs generated during the decay process, while properly incorporating the potential bias into the equation of motion of the DW. However, this is computationally challenging because with a constant bias, the DWs begin to collapse before it follows the scaling solution, necessitating the aforementioned simplification.

In our scenario, the bias is temperature dependent. In particular, the bias is almost negligible initially, allowing the DW to collapse within the numerical time frame after following the scaling solution. Consequently, we are able to evaluate the generation of GWs during the DW decay process, including the effect of the bias, in the numerical lattice calculations. This allows us to accurately estimate the GW spectrum and make a valid comparison between the observed pulsar timing data and the theoretical prediction. This is exactly the purpose of this paper.

We comment here on the relevant literature in the past. Axion DWs or string-wall networks that collapse due to the potential bias arising from the non-perturbative QCD effect were considered in Refs. [16, 17]. In particular, it was pointed out in Ref. [17] that the annihilation of axion string-DW network produces GWs in the nanohertz range. The setup was motivated by the so-called clockwork QCD axion model [26], where there are

several heavy axions coupled to QCD. These heavy axions can be searched for in accelerator experiments [16, 17]. A similar scenario with axion DWs coupled to QCD was also recently discussed in Ref. [18], where the implications for the observed data of the pulsar timing array, as well as various collider and beam-dump experiments, were studied in detail. This paper differs from previous studies by introducing a temperature-dependent bias in the process of solving for the evolution of DWs on the lattice and evaluating the GWs generated during the DW decay process. This approach allows for a more accurate prediction of the GW spectrum produced by the decay of axion DWs coupled to QCD. We will see that the predicted spectrum agrees very well with the recently published pulsar timing data [19–21].

The rest of this paper is structured as follows. In Sec. 2, we provide a brief review of domain walls in axion theory and present our setup. In Sec. 3, we elaborate on DW annihilation and GW emission, and display the numerical results for the GW spectrum. The final section is devoted to discussion and conclusion.

2 Axion domain walls

Let us here introduce the axion, ϕ , as a field satisfying the periodic condition,

$$\phi \rightarrow \phi + 2\pi f_\phi, \quad (1)$$

where f_ϕ is the decay constant. The action is exactly invariant under this translation. Since the potential remains also invariant under the shift, we must have degenerate vacua at $\phi = \langle \phi \rangle$ and $\phi = \langle \phi \rangle + 2\pi f_\phi$. Thus there is a DW configuration separating the two adjacent vacua. For instance, we may consider the axion potential of the simple cosine form,

$$V(\phi) = \frac{m_\phi^2 f_\phi^2}{n^2} \left(1 - \cos \left(n \frac{\phi}{f_\phi} \right) \right) \quad (2)$$

with n being a nonzero integer to satisfy Eq. (1). Here m_ϕ is the mass of the axion, and we assume $m_\phi \ll f_\phi$. Such a potential can be generated by some non-perturbative effects. Later we will introduce a coupling to QCD, which gives an additional contribution to the mass, but it is negligibly small and will be neglected in the following.

This potential has degenerate minima at $\phi = \frac{m}{n} 2\pi f_\phi$ with m being an integer. Thus, we have DW configurations where ϕ changes from $\frac{m}{n} \times 2\pi f_\phi$ to $\frac{1+m}{n} \times 2\pi f_\phi$. Each DW has a tension of

$$\sigma = \frac{8}{n^2} m_\phi f_\phi^2. \quad (3)$$

If we embed the axion in a phase of a complex scalar field as $\Phi = f_\phi/\sqrt{2}e^{i\phi/f_\phi}$, n is identified with the so-called DW number, which counts the number of different vacua. The shift symmetry of the axion is now identified with the Peccei-Quinn $U(1)_{\text{PQ}}$ symmetry of Φ . It is possible that Φ develops a nonzero vacuum expectation value at a certain point in the history of the universe, spontaneously breaking the $U(1)_{\text{PQ}}$ symmetry. Then, cosmic strings are formed. The axion potential (2) further breaks it down to the Z_n subgroup, leading to the formation of DWs. If $n = 1$, one DW is attached to each axion string, and the string-wall system becomes unstable due to the tension of DWs, and soon disappears after the formation of DWs. On the other hand, if $n \geq 2$, the string-wall system becomes long-lived.

Even if $n \geq 2$, the string-wall system becomes unstable if the degeneracy of the vacua is lifted by other contributions to the potential. A possible contribution to the potential could come from the interaction with the Standard Model particles. In particular, ϕ may couple to gluons through

$$\mathcal{L} \supset -\frac{\alpha_s}{8\pi} \left(n_{\text{mix}} \frac{\phi}{f_\phi} + \theta \right) G_{\mu\nu}^a \tilde{G}_a^{\mu\nu}, \quad (4)$$

where α_s is the strong coupling constant, G the gluon field strength, and \tilde{G} its dual. Here n_{mix} is another integer to satisfy Eq. (1), and θ is the strong CP phase. Through this coupling, the axion acquires the QCD-induced potential,

$$V_{\text{QCD}}(\phi) = \chi(T) \left[1 - \cos \left(n_{\text{mix}} \frac{\phi}{f_\phi} + \theta \right) \right], \quad (5)$$

where the topological susceptibility is given by

$$\chi(T) = \begin{cases} \chi_0 & (T < T_{\text{QCD}}) \\ \chi_0 \left(\frac{T}{T_{\text{QCD}}} \right)^{-c} & (T \geq T_{\text{QCD}}) \end{cases}. \quad (6)$$

Here, we adopt $c = 8.16$ [27], $\chi_0 = (75.6 \text{ MeV})^4$, and $T_{\text{QCD}} = 153 \text{ MeV}$. For instance with $n_{\text{mix}} = 1$ and $\theta = 0$, V_{QCD} has a true minimum at $\phi = 0$. For $n_{\text{mix}} \neq 1$, there are other minima if n_{mix} and n have a common divisor other than unity.

We consider a situation where some stable DW configurations, present at $T \gg T_{\text{QCD}}$, disappear at $T \sim T_{\text{QCD}}$ due to the potential bias V_{QCD} . In the following, we will mainly focus on the case of

$$n = 2, \quad n_{\text{mix}} = 1, \quad (7)$$

for simplicity of discussion. The potential shape is shown in Fig. 1, where the phase and height of the potentials are arbitrarily chosen, and the bias is exaggerated for illustration purpose. While the potential has degenerated minima at $T \gg T_{\text{QCD}}$, the degeneracy is lifted

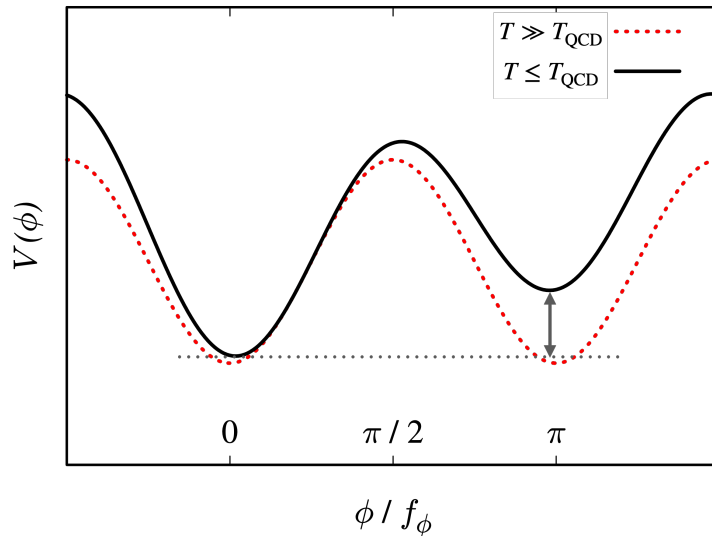


Figure 1: The potential shape for $n_{\text{mix}} = 1$ and $n = 2$. The red dotted and black solid lines denote the case with $T \gg T_{\text{QCD}}$, and $T \leq T_{\text{QCD}}$, respectively.

by V_{QCD} at $T \leq T_{\text{QCD}}$. The difference in the potential at two local minima, or simply the bias, varies from 0 to $2\chi_0$ depending on θ in the case of $n = 2$ and $n_{\text{mix}} = 1$, but its typical value is of order χ_0 .

3 Collapse of DW network and GWs, precisely

The DWs start to annihilate when the bias becomes comparable to the DW energy density. Following the earlier studies, we use

$$\mathcal{F} \times \chi(T_{\text{eq}}) = H(T_{\text{eq}})\sigma, \quad (8)$$

to define T_{eq} as the cosmic temperature when the tension and the potential bias become equal to each other. Here \mathcal{F} is an $\mathcal{O}(1)$ constant that accounts for the θ and n_{mix} dependence. For simplicity, we assume $\mathcal{F} = 1$ in the following. Note that it takes some more time for most of the DWs to annihilate due to the bias. We define the temperature at which most of the DWs annihilate by T_{ann} , which is different from T_{eq} as we will see.

We note that, compared to the usual biased DW, we have a time dependence in the bias $\chi(T)$. This means that as long as $\chi(T_{\text{QCD}}) \gtrsim H(T_{\text{QCD}})\sigma$, namely $\sigma \lesssim 2 \times 10^{15} \text{ GeV}^3$,

the DWs will start to annihilate around the QCD scale. In addition, it is not allowed that $\sigma \gg 2 \times 10^{15} \text{ GeV}^3$; otherwise, the DW dominates the Universe and a false vacuum eternal inflation may occur. Thus,

$$\sigma \lesssim 10^{15} \text{ GeV}^3 \quad (9)$$

is the phenomenologically allowed region in our scenario.¹ This means that the DWs must start to annihilate around

$$T_{\text{eq}} \sim 0.1 \text{ GeV}. \quad (10)$$

3.1 Analytic approach to the GW spectrum

Following Ref. [10], we first assume that the DWs instantaneously annihilate at $T = T_{\text{eq}}$, i.e., $T_{\text{ann}} = T_{\text{eq}}$ although we will see that this assumption is invalid in our numerical result. Even before the DWs annihilate, the DWs are decaying in the scaling regime. The energy of the decaying DWs is released to the axion particles and GWs. The spectrum of the GWs emitted from the decaying DWs has a peak corresponding to the Hubble parameter at the DW decay. Since the energy fraction of the DWs increases in the scaling regime, the peak of the current GW spectrum is determined by the Hubble parameter at the DW annihilation,

$$f_{\text{peak}} \sim H(T_{\text{eq}}). \quad (11)$$

Taking into account the redshift of the peak frequency due to the cosmic expansion, one obtains the present value of the peak frequency as

$$f_{\text{peak},0} \simeq 13 \text{ nHz} \times \left(\frac{g_*(T_{\text{eq}})}{20} \right)^{1/6} \left(\frac{T_{\text{eq}}}{0.1 \text{ GeV}} \right). \quad (12)$$

Here, $g_*(T)$ is the relativistic degree of freedom for the energy density.

The peak value of Ω_{GW} at the DW annihilation can be estimated as

$$\Omega_{\text{GW,ann}}^{\text{peak}} = \left. \frac{\tilde{\epsilon}_{\text{GW}} \mathcal{A}^2 \sigma^2}{24\pi M_{\text{pl}}^4 H^2} \right|_{T=T_{\text{eq}}}, \quad (13)$$

where $\tilde{\epsilon}_{\text{GW}} \simeq 0.7 \pm 0.4$ [10] parametrizes the efficiency of GW emission and \mathcal{A} is the so-called area parameter defined by $\rho_{\text{DW}} = \mathcal{A}\sigma/t$. When $T \simeq T_{\text{eq}}$, the area parameter is $\mathcal{O}(1)$ and the bias is comparable to the DW density, i.e., $\rho_{\text{DW}} \sim \chi(T_{\text{eq}})$. Then we get

$$\Omega_{\text{GW,ann}}^{\text{peak}} = \left. \frac{\xi^2 \chi^2}{24\pi M_{\text{pl}}^4 H^4} \right|_{T=T_{\text{eq}}}. \quad (14)$$

¹From an anthropic point of view, it may be preferable for the tension to saturate the bound.

Here, we have introduced a parameter ξ to include various numerical factors such as the θ dependence of bias, the area parameter, and the efficiency of the GW emission. The present value of Ω_{GW} has a peak of

$$\Omega_{\text{GW},0}^{\text{peak}} h^2 = \Omega_r h^2 \frac{g_{\star}(T_{\text{eq}})}{g_{\star,0}} \left(\frac{g_{\star s,0}}{g_{\star s}(T_{\text{eq}})} \right)^{4/3} \Omega_{\text{GW,ann}}^{\text{peak}}, \quad (15)$$

where $\Omega_r h^2 = 4.15 \times 10^{-5}$ is the density parameter of radiation, and $g_{\star s}(T)$ is the relativistic degree of freedom for the entropy density. Thus, we get

$$\Omega_{\text{GW},0}^{\text{peak}} h^2 \simeq 2.7 \times 10^{-10} \left(\frac{g_{\star s}(T_{\text{eq}})}{20} \right)^{-4/3} \left(\frac{g_{\star}(T_{\text{eq}})}{20} \right)^{-1} \xi^2 \begin{cases} \left(\frac{T_{\text{QCD}}}{T_{\text{eq}}} \right)^{8+2c} & (T_{\text{eq}} < T_{\text{QCD}}) \\ \left(\frac{T_{\text{QCD}}}{T_{\text{eq}}} \right)^8 & (T_{\text{eq}} \geq T_{\text{QCD}}) \end{cases}, \quad (16)$$

where we used $g_{\star,0} = 3.36$ and $g_{\star s,0} = 3.91$. For the shape of $\Omega_{\text{GW},0}$ away from the peak, numerical simulations show the frequency dependence as $\Omega_{\text{GW}} \propto f^3$ for low frequency and $\Omega_{\text{GW}} \propto f^{-1}$ for high frequency [10].

3.2 Numerical approach and GW, precisely

So far, we have assumed that the DWs instantaneously annihilate at $T = T_{\text{eq}}$. However, the DW annihilation delays compared to the balance between the bias and the DW tension in realistic situations. In this case, the peak frequency of the GW spectrum shifts to lower frequencies, and the peak abundance is also modified. We parameterize the delay of the annihilation by a factor $C(\leq 1)$ defined by

$$T_{\text{ann}} = CT_{\text{eq}}. \quad (17)$$

Then, the peak frequency is given by

$$f_{\text{peak},0} \simeq 13 \text{ nHz} \times \left(\frac{g_{\star}(T_{\text{ann}})}{20} \right)^{1/6} \left(\frac{T_{\text{ann}}}{0.1 \text{ GeV}} \right), \quad (18)$$

$$= 13 \text{ nHz} \times C \left(\frac{g_{\star}(T_{\text{ann}})}{20} \right)^{1/6} \left(\frac{T_{\text{eq}}}{0.1 \text{ GeV}} \right). \quad (19)$$

The peak abundance is modified by two effects; one is the delay of the annihilation, which leads to an increase in the peak abundance, and the other is the deviation from the scaling regime, which leads to a decrease in the peak abundance. We represent the modification of $\Omega_{\text{GW},0}^{\text{peak}}$ by a change in ξ .

We have performed the lattice calculation to numerically simulate the annihilation of the DWs with a time-varying bias and evaluated the GW spectrum based on the analysis in Ref. [28]. We find $C \approx 0.4$ and $\xi^2 \approx 19$. See the Appendix for more details. We show the GW spectrum from the DW annihilations for $T_{\text{eq}} = 1.07T_{\text{QCD}}$ in Fig. 2, where we have used $g_\star = g_{\star s} = 10.75$ to obtain the current GW spectrum. The solid red line represents the numerical result of the lattice simulation.² Here, we assign a numerical uncertainty of a factor of 2 to the numerical result and show it as a red-shaded region. For comparison, we also show the analytic formulae assuming $T_{\text{eq}} = T_{\text{ann}}$, Eqs. (12) and (16), with $\xi = 1$. We can see that the spectrum obtained by numerical calculations has a higher peak at a lower frequency compared to the analytic formulae. The obtained spectrum matches well to the GW spectrum for the domain wall decaying into the Standard Model particles fitted to the NANOGrav 15 yr dataset [25]. Since the GW strains reported by the EPTA [20], PPTA [21], and CPTA [22] groups show a similar trend to that of the NANOGrav, the GW spectrum in our scenario also matches them in the range of the uncertainties with a slight change in T_{eq} .

This also gives that for the desired amplitude of the GW, we need to have $\sigma \sim 10^{15} \text{ GeV}^3$, which gives the parameter region in mass and decay constant plane. In particular, using Eq. (8), we obtain

$$\sigma \simeq 1.1 \times 10^{15} \text{ GeV}^3 \times \left(\frac{g_\star(T_{\text{eq}})}{20} \right)^{-1/2}, \quad (20)$$

for $T_{\text{eq}} = 1.07T_{\text{QCD}}$. This is shown in Fig. 3 in $m_\phi - f_\phi^{-1}$ plane. Here we show the parameter region of $\sigma \sim 10^{14-16} \text{ GeV}^3$, which is suggested by the NANOGrav. We notice that in our model, the axion must couple to the gluon, and we adopted some constraints and future reaches from the paper [31], which translates the ones from Ref. [32]. In addition, for the big-bang nucleosynthesis (BBN) bound with $m_\phi > 0.2 \text{ GeV}$, we require the lifetime of the axion to be shorter than 0.01 s as a conservative bound, since the axion produced from the DW annihilation has a different spectrum from the ones produced thermally (we also have thermally produced component, see e.g., Ref. [33] for the bound in this case). One can see that there are large parameter regions that are consistent with the NANOGrav data. Indeed, we can have at most $m_\phi \sim f_\phi$ from the perturbativity. Some of the parameter regions can be probed in the future/recent accelerator experiments. They can confirm our scenario.

²We take the values of g_\star and $g_{\star s}$ for the cosmic temperature around 10 MeV because of the delay of the annihilation. Even for a slightly larger one, we can have equally good fit by slightly decreasing T_{eq} by $\mathcal{O}(1)\%$.

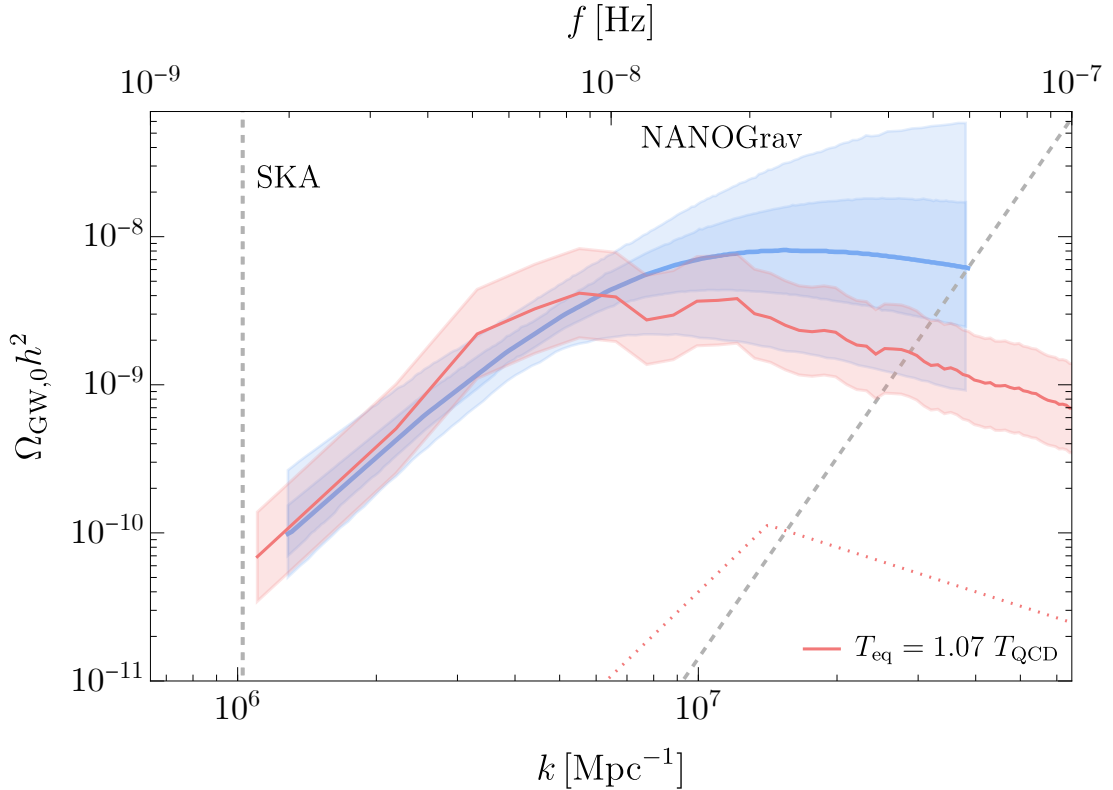


Figure 2: GW spectrum from the DW annihilations for $T_{\text{eq}} = 1.07 T_{\text{QCD}}$. The red solid line is the result of the numerical simulation and the red dotted line represents the fitting formula for a constant bias. We also show the numerical uncertainty as the red-shaded region which is set to be a factor of 2. The blue line is the median GW spectrum from the DW network decaying in the standard model particles for the NANOGraV 15 yr dataset [25]. The blue-shaded regions correspond to the 68% and 95% regions. The gray dashed line shows the future sensitivity of SKA [29], which is evaluated following Ref. [30].

We also mention that recently the DW network without strings, with initial inflationary fluctuation, was shown to be rather stable against the population bias [46]. In this case, we have the desired GW as well without significantly changing our arguments. The resultant GW spectrum is expected to be broader, and we may have a better fit to the NANOGraV data or other PTA data which favors a mild dependence of the spectrum on the frequency. (See more details in Ref. [28].)

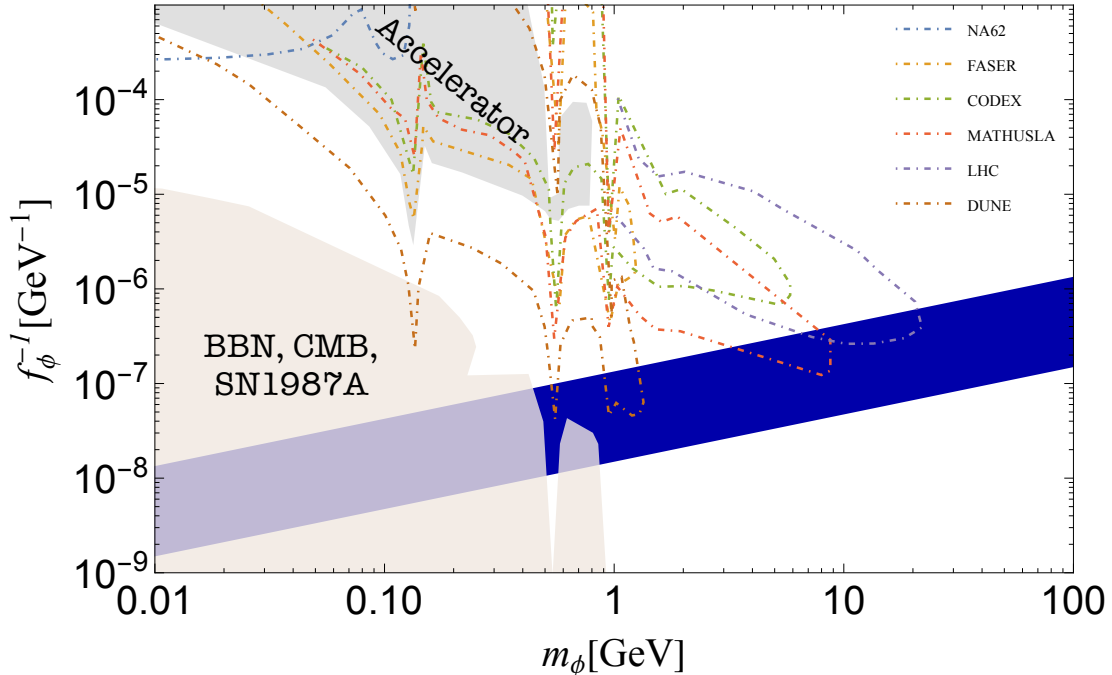


Figure 3: The predicted parameter region of our scenario for the correct amplitude of the GW is shown in $m_\phi - f_\phi^{-1}$ plane in the blue band with $n_{\text{mix}} = 1, n = 2$. Various bounds and reaches are adopted from Ref. [31]. We used the expected reaches of various experiments such as CODEX, DUNE, FASER, LHC, MATHUSLA, and NA62 [32, 34–39] as well as the cosmological and astrophysical bounds [40–44]. See also Ref. [45] for certain theoretical uncertainties of the estimated experimental reaches. The BBN bound for $m_\phi > 0.2 \text{ GeV}$ is set by requiring the lifetime of the axion to be shorter than 0.01 s.

4 Conclusions and discussion

Primordial black hole formation In our scenario, the primordial black hole (PBH) may be formed because, around the DW annihilation, the false vacuum energy surrounded by a DW bubble is not very small compared to the radiation energy density, which dominates the Universe. If such a false vacuum bubble has a radius comparable to the Schwarzschild radius, the bubble collapses to form a PBH (see e.g., Ref. [47]). A further study for the correct estimation of the volume fractions of the false vacuum evolution in late time at $T \ll T_{\text{eq}}$, the shape of the DWs, and angular momenta etc, will be important to estimate the abundance of the PBHs.

On the other hand, we also expect that the PBH formation should be more likely in

the case of the DWs with initial inflationary fluctuations. In this case, DW network has large voids [46], which easily lead to large false vacuum bubbles, which collapse after a long time due to the potential and population bias, and form PBHs [28]. In this case, we need to be careful of the isocurvature constraint, because the DW network also has an almost scale-invariant power spectrum [46] (See also Ref. [28]), and so does the resulting PBHs.

The prediction in our scenario is that, if PBHs are formed from the DW collapse, the PBH mass should be around M_{\odot} since DWs annihilate around the QCD scale. These PBHs may explain the LIGO/VIRGO events [48–51] (see also Refs. [52–54]).

Strong CP problem Let us address the strong CP problem in this part. We can solve the strong CP problem in this scenario in several ways. One is that the phase is tuned to be small, i.e., $|\langle\phi\rangle/f_{\phi} + \theta| \ll 10^{-10}$ to be consistent with the neutron electric dipole moment bound. This is possible if ϕ is a heavy QCD axion. Alternatively, it may be related to the inflation dynamics [31] (see also Ref. [55], in which case we need to consider the light axion dynamics as in the following discussion.)

We may also have another usual QCD axion to drive the strong CP phase after the DW annihilation to zero. This is the case that the QCD axion is light enough, namely the decay constant $f_a \gtrsim 10^{17}$ GeV (see Refs. [56, 57] for explaining the abundance without fine-tuning). If the QCD axion is relatively heavy and starts to oscillate before the DW annihilation, the evolution becomes more non-trivial. The QCD axion oscillates around the different vacua in different domains during the DW scaling solution. In this case, the PBHs or miniclusters can be formed due to another mechanism called the QCD axion bubbles because, in the false vacuum surrounded by DWs, the axion oscillates around a different minimum (c.f. Ref. [58]). This effect may be dominant if the annihilation happens at a higher temperature with a smaller bias and tension of the DWs, and thus the previously mentioned PBH formation is suppressed. We also note that in order to have this DW formation, the QCD axion should not start to oscillate much earlier than the time of the DW annihilation with a bias of $\chi(T)$. Otherwise, the vacua in both domains will have the same vacuum energy around which the QCD axion oscillates (with different amplitudes). So we need the condition that the potential bias effect induces such efficient DW annihilation. This implies that the bias becomes important just before the onset of the oscillation.

Conclusions We have shown that the recently reported NANOGrav, EPTA, PPTA, and CPTA data can be explained by the axionic domain wall coupled to the QCD gluons. In this case, the DW bias is obtained at the cosmic temperature around the QCD phase transition,

and it naturally explains the frequency of the pulsar timing data. We have carefully studied the GW spectrum by performing the lattice simulations taking account of the time dependence of the bias and shown the stochastic gravitational waves in the nanohertz region. Our scenario may be probed in future accelerator experiments. We also commented that PBHs of around a solar mass may also be formed due to the DW collapse, and it may explain LIGO/Virgo black merger events.

Acknowledgments

This work is supported by JSPS Core-to-Core Program (grant number: JPJSCCA20200002) (F.T.), JSPS KAKENHI Grant Numbers 23KJ0088 (K.M.), 20H01894 (F.T. and N.K.), 20H05851 (F.T., W.Y., and N.K.), 21K20364 (W.Y.), 22K14029 (W.Y.), and 22H01215 (W.Y.), 21H01078 (N.K.), 21KK0050 (N.K.), Graduate Program on Physics for the Universe (J.L.). This article is based upon work from COST Action COSMIC WISPerS CA21106, supported by COST (European Cooperation in Science and Technology).

A Numerical simulation

Here we explain the setup for the lattice simulation. The analysis here is based on Ref. [28]. We use 1024^3 lattice of the ϕ^4 theory (see Refs. [46, 59] for the setup) with the box that initially contains 50^3 Hubble horizons. The potential is given by

$$V(\phi) = V_0 - \frac{1}{2}m_0^2\phi^2 + \frac{\lambda}{4}\phi^4. \quad (21)$$

We also define the vacuum expectation value, v , of $|\phi|$ by $m_0^2 = \lambda v^2$. The scale factor $a(t)$ is set to be unity when $H = m_0$. We evolve the conformal time τ in the range $(1-8)/m_0$. We stop the simulation at $\tau = 8/m_0$ because the Lorentz contracted domain wall width cannot be resolved for $\tau \gg 8/m_0$ in our simulation.³ Here the conformal time is normalized by the mass scale m_0 such that the Hubble parameter at the initial time is equal to m_0 . To mimic the QCD potential, we put a time-dependent potential bias

$$V_{\text{bias}}(\tau) = \lambda v^3 \phi \times b(\tau), \quad (22)$$

$$b(\tau) \equiv \frac{\epsilon}{1 + e^{-2(\tau-\tau')/\Delta\tau}}. \quad (23)$$

³We have checked at the end of estimation that the volume fraction of the false vacuum is smaller than 10%.

Here $\epsilon = 0.05$, $\tau' = 4/m_0$, $\Delta\tau = 0.2/m_0$, and $a(\tau = 1/m_0) = 1$. We assume radiation dominated Universe. Analytically one finds that $H\sigma = 2\lambda v^4 b(\tau)$ happens at the time $\tau \simeq 4.03/m_0$ at which the temperature is defined as T_{eq} . The analytic form is obtained by replacing χ by $2\lambda v^4 b(\tau)$. Therefore the peak frequency from Eq. (11) corresponds to the comoving $k_{\text{peak}} = 1.56m_0$ (note that $f_{\text{peak}} = k_{\text{peak}}/(2\pi)$). The peak height from Eq. (14) with $\xi = 1$ corresponds to $\sim 0.78(v/M_{\text{pl}})^4$. One can see from Fig. 4, that the peak position is lower than the analytic form by a factor of 2.5, i.e., $C \approx 0.4$, while the peak position is ~ 19 times higher than the analytic form, i.e., $\xi^2 \approx 19$. The relation between the numerical estimate and the analytic one is used to map the numerical result in the main part, where we introduced some numerical uncertainty factors. The bias has a different form from the realistic QCD-induced potential for alleviating the numerical cost. This difference is also the systematic uncertainty.

We also checked that the ratio of the numerical result to the analytic one for the peak position and height has $\mathcal{O}(1)$ uncertainty depending on the parameter choice. Thus we expect

$$C = \mathcal{O}(0.1), \quad \xi^2 = \mathcal{O}(10). \quad (24)$$

We note that in our analysis we did not include the axion strings to simplify the analysis. We believe that this is a fairly good approximation when $N_{\text{DW}} = 2$, because two domain walls attached to a single string can be approximated by a single domain wall.

References

- [1] Y. B. Zeldovich, I. Y. Kobzarev, and L. B. Okun, *Zh. Eksp. Teor. Fiz.* **67**, 3 (1974).
- [2] T. W. B. Kibble, *J. Phys. A* **9**, 1387 (1976).
- [3] A. Vilenkin, *Phys. Rev. D* **23**, 852 (1981).
- [4] A. Vilenkin and E. P. S. Shellard, *Cosmic Strings and Other Topological Defects* (Cambridge University Press, 2000).
- [5] J. Preskill, S. P. Trivedi, F. Wilczek, and M. B. Wise, *Nucl. Phys. B* **363**, 207 (1991).
- [6] S. Chang, C. Hagmann, and P. Sikivie, *Phys. Rev. D* **59**, 023505 (1999), [arXiv:hep-ph/9807374](https://arxiv.org/abs/hep-ph/9807374).
- [7] M. Gleiser and R. Roberts, *Phys. Rev. Lett.* **81**, 5497 (1998), [arXiv:astro-ph/9807260](https://arxiv.org/abs/astro-ph/9807260).

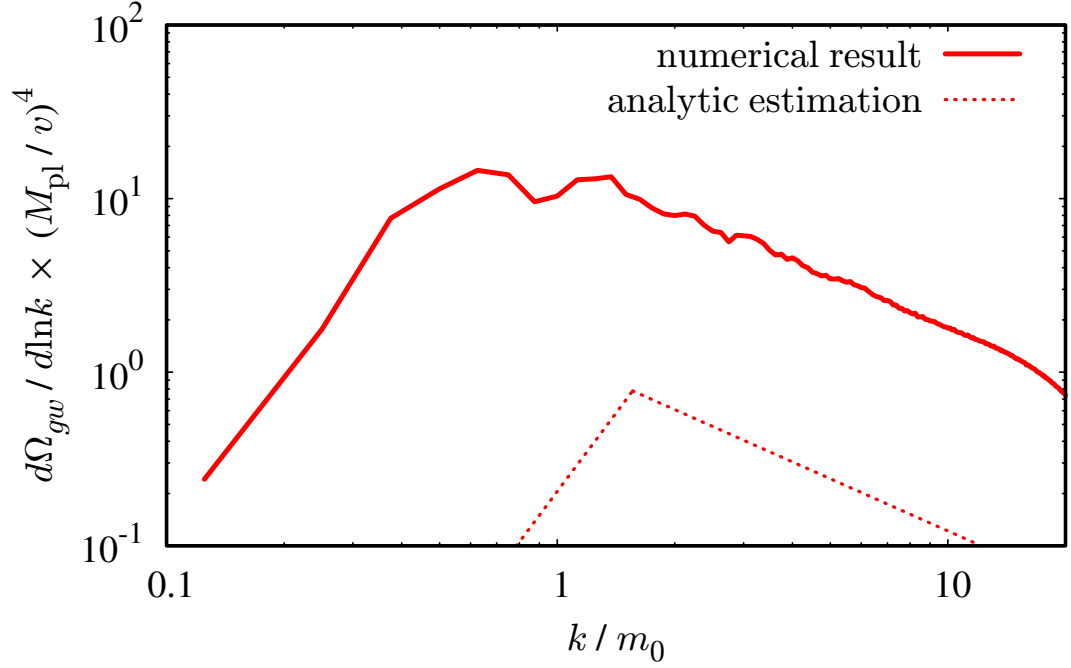


Figure 4: Numerical result of GW spectrum from the DW annihilations in terms of the comoving momentum normalized by the mass, k/m_0 . See the text.

- [8] T. Hiramatsu, M. Kawasaki, and K. Saikawa, *JCAP* **05**, 032 (2010), [arXiv:1002.1555 \[astro-ph.CO\]](#) .
- [9] M. Kawasaki and K. Saikawa, *JCAP* **09**, 008 (2011), [arXiv:1102.5628 \[astro-ph.CO\]](#) .
- [10] T. Hiramatsu, M. Kawasaki, and K. Saikawa, *JCAP* **02**, 031 (2014), [arXiv:1309.5001 \[astro-ph.CO\]](#) .
- [11] K. Nakayama, F. Takahashi, and N. Yokozaki, *Phys. Lett. B* **770**, 500 (2017), [arXiv:1612.08327 \[hep-ph\]](#) .
- [12] K. Saikawa, *Universe* **3**, 40 (2017), [arXiv:1703.02576 \[hep-ph\]](#) .
- [13] F. Takahashi, T. T. Yanagida, and K. Yonekura, *Phys. Lett. B* **664**, 194 (2008), [arXiv:0802.4335 \[hep-ph\]](#) .
- [14] M. Dine, F. Takahashi, and T. T. Yanagida, *JHEP* **07**, 003 (2010), [arXiv:1005.3613 \[hep-th\]](#) .

- [15] J. Jaeckel, V. V. Khoze, and M. Spannowsky, *Phys. Rev. D* **94**, 103519 (2016), [arXiv:1602.03901 \[hep-ph\]](#) .
- [16] T. Higaki, K. S. Jeong, N. Kitajima, and F. Takahashi, *JHEP* **06**, 150 (2016), [arXiv:1603.02090 \[hep-ph\]](#) .
- [17] T. Higaki, K. S. Jeong, N. Kitajima, T. Sekiguchi, and F. Takahashi, *JHEP* **08**, 044 (2016), [arXiv:1606.05552 \[hep-ph\]](#) .
- [18] R. Z. Ferreira, A. Notari, O. Pujolas, and F. Rompineve, *JCAP* **02**, 001 (2023), [arXiv:2204.04228 \[astro-ph.CO\]](#) .
- [19] G. Agazie *et al.* (NANOGrav), (2023), [10.3847/2041-8213/acdac6](#), [arXiv:2306.16213 \[astro-ph.HE\]](#) .
- [20] J. Antoniadis *et al.*, (2023), [arXiv:2306.16214 \[astro-ph.HE\]](#) .
- [21] D. J. Reardon *et al.*, (2023), [10.3847/2041-8213/acdd02](#), [arXiv:2306.16215 \[astro-ph.HE\]](#) .
- [22] H. Xu *et al.*, (2023), [10.1088/1674-4527/acdfa5](#), [arXiv:2306.16216 \[astro-ph.HE\]](#) .
- [23] Y. Nakai, M. Suzuki, F. Takahashi, and M. Yamada, *Phys. Lett. B* **816**, 136238 (2021), [arXiv:2009.09754 \[astro-ph.CO\]](#) .
- [24] W. Ratzinger and P. Schwaller, *SciPost Phys.* **10**, 047 (2021), [arXiv:2009.11875 \[astro-ph.CO\]](#) .
- [25] A. Afzal *et al.* (NANOGrav), (2023), [10.3847/2041-8213/acdc91](#), [arXiv:2306.16219 \[astro-ph.HE\]](#) .
- [26] T. Higaki, K. S. Jeong, N. Kitajima, and F. Takahashi, *Phys. Lett. B* **755**, 13 (2016), [arXiv:1512.05295 \[hep-ph\]](#) .
- [27] S. Borsanyi *et al.*, *Nature* **539**, 69 (2016), [arXiv:1606.07494 \[hep-lat\]](#) .
- [28] J. Lee, N. Kitajima, F. Takahashi, and W. Yin, in preparation (2023).
- [29] G. Janssen *et al.*, *PoS AASKA14*, 037 (2015), [arXiv:1501.00127 \[astro-ph.IM\]](#) .
- [30] K. Inomata and T. Nakama, *Phys. Rev. D* **99**, 043511 (2019), [arXiv:1812.00674 \[astro-ph.CO\]](#) .

- [31] F. Takahashi and W. Yin, *JCAP* **10**, 057 (2021), [arXiv:2105.10493 \[hep-ph\]](#) .
- [32] K. J. Kelly, S. Kumar, and Z. Liu, *Phys. Rev. D* **103**, 095002 (2021), [arXiv:2011.05995 \[hep-ph\]](#) .
- [33] P. F. Depta, M. Hufnagel, and K. Schmidt-Hoberg, *JCAP* **05**, 009 (2020), [arXiv:2002.08370 \[hep-ph\]](#) .
- [34] J. P. Chou, D. Curtin, and H. J. Lubatti, *Phys. Lett. B* **767**, 29 (2017), [arXiv:1606.06298 \[hep-ph\]](#) .
- [35] V. V. Gligorov, S. Knapen, M. Papucci, and D. J. Robinson, *Phys. Rev. D* **97**, 015023 (2018), [arXiv:1708.09395 \[hep-ph\]](#) .
- [36] J. L. Feng, I. Galon, F. Kling, and S. Trojanowski, *Phys. Rev. D* **98**, 055021 (2018), [arXiv:1806.02348 \[hep-ph\]](#) .
- [37] A. Ariga *et al.* (FASER), *Phys. Rev. D* **99**, 095011 (2019), [arXiv:1811.12522 \[hep-ph\]](#) .
- [38] A. Hook, S. Kumar, Z. Liu, and R. Sundrum, *Phys. Rev. Lett.* **124**, 221801 (2020), [arXiv:1911.12364 \[hep-ph\]](#) .
- [39] G. Aielli *et al.*, *Eur. Phys. J. C* **80**, 1177 (2020), [arXiv:1911.00481 \[hep-ex\]](#) .
- [40] M. I. Vysotsky, Y. B. Zeldovich, M. Y. Khlopov, and V. M. Chechetkin, *Pisma Zh. Eksp. Teor. Fiz.* **27**, 533 (1978).
- [41] G. G. Raffelt, *Lect. Notes Phys.* **741**, 51 (2008), [arXiv:hep-ph/0611350](#) .
- [42] D. Cadamuro and J. Redondo, *JCAP* **02**, 032 (2012), [arXiv:1110.2895 \[hep-ph\]](#) .
- [43] M. Millea, L. Knox, and B. Fields, *Phys. Rev. D* **92**, 023010 (2015), [arXiv:1501.04097 \[astro-ph.CO\]](#) .
- [44] P. A. Zyla *et al.* (Particle Data Group), *PTEP* **2020**, 083C01 (2020).
- [45] P. Agrawal *et al.*, *Eur. Phys. J. C* **81**, 1015 (2021), [arXiv:2102.12143 \[hep-ph\]](#) .
- [46] D. Gonzalez, N. Kitajima, F. Takahashi, and W. Yin, (2022), [arXiv:2211.06849 \[hep-ph\]](#) .
- [47] F. Ferrer, E. Masso, G. Panico, O. Pujolas, and F. Rompineve, *Phys. Rev. Lett.* **122**, 101301 (2019), [arXiv:1807.01707 \[hep-ph\]](#) .

- [48] B. P. Abbott *et al.* (LIGO Scientific, Virgo), *Phys. Rev. Lett.* **116**, 061102 (2016), [arXiv:1602.03837 \[gr-qc\]](#) .
- [49] B. P. Abbott *et al.* (LIGO Scientific, Virgo), *Phys. Rev. Lett.* **116**, 241103 (2016), [arXiv:1606.04855 \[gr-qc\]](#) .
- [50] B. P. Abbott *et al.* (LIGO Scientific, VIRGO), *Phys. Rev. Lett.* **118**, 221101 (2017), [Erratum: *Phys.Rev.Lett.* 121, 129901 (2018)], [arXiv:1706.01812 \[gr-qc\]](#) .
- [51] B. P. Abbott *et al.* (LIGO Scientific, Virgo), *Phys. Rev. Lett.* **119**, 141101 (2017), [arXiv:1709.09660 \[gr-qc\]](#) .
- [52] S. Bird, I. Cholis, J. B. Muñoz, Y. Ali-Haïmoud, M. Kamionkowski, E. D. Kovetz, A. Raccanelli, and A. G. Riess, *Phys. Rev. Lett.* **116**, 201301 (2016), [arXiv:1603.00464 \[astro-ph.CO\]](#) .
- [53] S. Clesse and J. García-Bellido, *Phys. Dark Univ.* **15**, 142 (2017), [arXiv:1603.05234 \[astro-ph.CO\]](#) .
- [54] M. Sasaki, T. Suyama, T. Tanaka, and S. Yokoyama, *Phys. Rev. Lett.* **117**, 061101 (2016), [Erratum: *Phys.Rev.Lett.* 121, 059901 (2018)], [arXiv:1603.08338 \[astro-ph.CO\]](#) .
- [55] F. Takahashi and W. Yin, (2023), [arXiv:2301.10757 \[hep-ph\]](#) .
- [56] P. W. Graham and A. Scherlis, *Phys. Rev. D* **98**, 035017 (2018), [arXiv:1805.07362 \[hep-ph\]](#) .
- [57] F. Takahashi, W. Yin, and A. H. Guth, *Phys. Rev. D* **98**, 015042 (2018), [arXiv:1805.08763 \[hep-ph\]](#) .
- [58] N. Kitajima and F. Takahashi, *JCAP* **11**, 060 (2020), [arXiv:2006.13137 \[hep-ph\]](#) .
- [59] N. Kitajima, F. Kozai, F. Takahashi, and W. Yin, *JCAP* **10**, 043 (2022), [arXiv:2205.05083 \[astro-ph.CO\]](#) .